RESEARCH PAPER

"Formulation and Characterization of Artemether-Gellan Gum Nanoparticles for Treatment of Malaria: Factorial Design Approach"

Mrs. Harshali Sanjay Jadhav[1], Dr. Gaurav Jain[2], Dr. Phool Singh Yaduwanshi[3]

[1]Research Scholar, IES Institute of Pharmacy, IES University, Bhopal, Madhya Pradesh, India.
Email:ID: harshalijadhav1593@gmail.com
[2]Professor, IES Institute of Pharmacy, IES University, Bhopal, Madhya Pradesh, India.
Email:ID: gauravjain20us@gmail.com
[3]IES Institute of Technology & Management IES University, Bhopal, Madhya Pradesh, India.
Email:ID: phoolsinghyaduwanshi@gmail.com
Corresponding Author
Mrs. Harshali Sanjay Jadhav
Research Scholar, IES Institute of Pharmacy, IES University, Bhopal, Madhya Pradesh, India.
Email:ID: harshalijadhav1593@gmail.com

ABSTRACT
Background: Malaria is a global health priority with more than 3 billion people at risk. Resistance to all known classes of antimalarial develops and spreads quickly, making it difficult to treat malaria effectively. Artemether, one of the first antimalarial medications it works better against parasites that are resistant to other medications. The conventional dosage form of Artemether needs frequent dosing.
Objectives: Preparation of sustained release Artemether-Gellan gum nanoparticles (AM-NPs) to avoid frequent dosing.
Materials and Methods: Artemether-gellan gum nanoparticles were prepared using emulsion cross-linking method. The gellan gum concentration and polyvinyl alcohol concentration were optimized using 3-level 2-factor design process. The prepared Artemether-gellan gum nanoparticles were evaluated by using Fourier transform-infrared (FTIR), Differential scanning colorimetry (DSC), Particle size and zeta potential, X-ray Diffraction, and *In Vitro* Drug Release.
Results: All formulations had drug entrapment efficiencies between 82.98 and 91.78%. AM-NPs FTIR and DSC thermograms show no interaction. The prepared AM-NPs are shown to be in an amorphous condition by the XRD peaks. The improved formulation's zeta potential of -15.8 (mV) suggests good stability. Over a 12-hour period, the drug release of all 13 produced AM-NPs ranges from 87.09 to 98.26 percent.
Conclusion: The prepared formulation of Artemether-gellan gum nanoparticles offer 12-hour sustained release effect and solve frequent Artemether dosing issues
Keywords: Artemether; QbD; 3^2 factorial design; Nanoparticles; Sustained drug delivery etc
How to cite this article: Jadhav HS, Jain G, Yaduwanshi PS, "Formulation and Characterization of Artemether-Gellan Gum Nanoparticles for Treatment of Malaria: Factorial Design Approach", Int J Drug Deliv Technol. 2026;16(73s): 1451-1461. DOI: 10.25258/ijddt.16.73s.154
Source of support: Nil.
Conflict of interest: Nil.

INTRODUCTION

Malaria is a global health priority with more than 3 billion people at risk. Resistance to all known classes of anti-malarial develops and spreads quickly, making it difficult to treat malaria effectively [1]. Additionally, because intracellular parasites are not specifically targeted, high dosages of treatment drugs are employed, which increases the likelihood of associated toxicities [2]. The structure, content, and function of the host erythrocyte cell membrane are significantly altered when the malaria parasite invades [3]. Plasmodium is the genus of parasitic protozoa, which are unicellular microorganisms that cause malaria. The parasites that cause malaria in humans are Plasmodium falciparum (malaria tropica), Plasmodium vivax (malaria tertian), *Plasmodium malariae*, and *Plasmodium ovale* (malaria quaterna). When an infected female Anopheles mosquito bites a person, the parasite enters the bloodstream and makes its way to the liver, where it matures and reproduces [4-5]. Several medications, such as quinine, quinidine, chloroquine, primaquine, halofantrine (a related quinolone), and pyrimethamine, have been used to treat malaria; however, the parasite has reportedly become resistant to most of these medications. For this reason, the WHO has recommended using artemisinin and its derivatives, such as dihydroartemisinin, artesinuate, arteether, artemether (ARTM), and lumefantrine [6-7].

Artemether, one of the first antimalarial medications, is still superior to more recent ones; in fact, it works better against parasites that are resistant to other medications [8]. Both P. falciparum and simple malaria have been shown to be significantly inhibited by it. Additionally, it has been shown to be quite beneficial in treating cerebral malaria [9]. Because of its weak water solubility and hepatic first pass

*Author for Correspondence: harshalijadhav1593@gmail.com

action, artemether has inconsistent and low oral absorption, making the oral route ineffective. It is a member of class II biopharmaceuticals, which have high permeability and poor solubility. It has a very short half-life of two to three hours. Because oral artemether requires a course of 24 pills over the course of three days, the dosing regimen is non-compliant [10]. Each dose consists of four tablets containing 20 milligrams of artemether. In addition to creating uncertainty, it also results in drug resistance that necessitates higher dosages, which eventually causes intracellular parasite damage and nonspecific targeting [11]. By combining biopolymers (chitosan and gellan gum) in nanoparticle form, a novel dosage form was created to address the shortcomings of traditional artemether delivery methods. Because it uses less artemether, this recently discovered dosage form may be less toxic and improve patient compliance by reducing the frequency of doses [12]. The most stable, efficient, and safe nanostructures are thought to be polymeric nanoparticles (PNs). Therapeutic approaches based on nanotechnology have frequently been applied to drug-specific delivery [13]. Drug loading is accelerated by nanocarriers' high surface area and modifiable physicochemical characteristics. In addition to locally increasing the concentration gradient and contributing to drug accumulation at local action and/or absorption sites, the decreased dimensions also improve bioavailability and lessen side effects [14]. Utilizing natural polymers in PNs increases their efficacy, reduces toxicity, and improves stability, making them less immunogenic, biocompatible, and biodegradable [15]. Gellan gum (GG) and other polymers have been shown to have a mucoadhesive ability. They are also non-toxic, biodegradable, biocompatible, and reasonably priced [16]. Pseudomonas elodea produces gellan gum, a linear anionic hydrophilic exopolysaccharide that is a very attractive polymer due to its stability, resistance, and capacity to form a hydrogel structure in the stomach's acidic environment [17]. This allows it to regulate the rates of drug release in the upper segments of the GIT [18-19]. Furthermore, GG's well-known mucoadhesive qualities and capacity to shield medications from early (chemical and enzymatic) degradation are crucial for managing drug release kinetics [20].

The current study set out to create and evaluate Artemether-gellan gum nanoparticles (AM-NPs) as an antimalarial treatment. Advanced statistical optimization approaches are a practical and methodically effective tool that improves the R&D process and speeds up the creation of dosage forms. In this work, the concentration of polymers was optimized using a 3^2-factorial design. Physicochemical properties were investigated, and the impacts of two factors (concentrations of gellan gum and polyvinyl alcohol) on drug release and entrapment efficiency were assessed. Entrapment efficiency, X-ray diffraction (XRD), Fourier transform infrared spectroscopy (FTIR), particle size measurement, and in vitro release profile were used to analyse the nanoparticles.

Materials and Methods:

Materials: Artemether (AM) was obtained as gift sample from Cadila Pharmaceutical Pvt. Ltd., Dholka, Ahmadabad, India. Gellan gum (GG) was also gifted by Meron lab, Kerala, India. Dioctyl sodium sulfosuccinate (AOT) and polyvinyl alcohol (PVA) was purchased from Sigma-Aldrich, Bangalore and Galaxy Chemicals, Gandhinagar, India respectively. All other chemicals used for analysis were of analytical grades.

Preparation of Artemether-Gellan gum Nanoparticles: Emulsion cross-linking was used to create Artemether-gellan gum nanoparticles [21]. In short, 50 mg of Artemether and 10 mg/ml of pure gellan gum were made in methanol and deionized water (pH 8.0), respectively. Sonication (Sonics, Vibracell, USA) was used to emulsify the solution with three milliliters of Tween 80 (10% w/v) over an ice bath for one minute. By sonicating the initial emulsion for three minutes over an ice bath, the secondary w/o/w emulsion was created in 15 milliliters of polyvinyl alcohol (% as given in table 1) aqueous solution. With constant stirring, a 5 ml, 60%, w/v aqueous calcium chloride solution was added gradually to the aforementioned emulsion. A rotary vacuum evaporator (Heidolph, Germany) was used to extract methylene chloride under vacuum, and the resulting nanoparticles were collected by centrifugation at 15,000 rpm for an hour. After two rounds of washing with deionized water, the nanoparticles were centrifuged to extract the unentrapped medication and PVA. The resulting pellet was lyophilized after being reconstituted with water [22-23]

Table 1. Design given by Software for formulation of AM-NPs:

Experimental run	Independent variable		Dependent variables	
	Gellan Gum concentration (X1) (%)	Polyvinyl alcohol concentration (X2) (%)	EE Y1 (%)	DR Y2 (%)
F1	0.1	3.5	88.42	91.87
F2	0.05	4	82.98	94.68
F3	0.15	3.5	90.14	91.39
F4	0.05	3	87.23	89.06
F5	0.1	3.5	87.44	96.22
F6	0.15	3	91.78	87.09
F7	0.1	3.5	90.67	89.28
F8	0.1	3.5	86.05	90.06
F9	0.05	3.5	88.93	92.65
F10	0.1	4	83.02	95.57
F11	0.15	4	89.44	98.26
F12	0.1	3	86.37	92.83
F13	0.1	3.5	89.66	94.28
Coded levels				
Independent variable		**Low level (-1)**	**Medium level (0)**	**High level (+1)**
X_1= Gellan Gum concentration (%)		0.05	0.1	0.15
X_2= Polyvinyl alcohol concentration (%)		3	3.5	4

Experimental design: Throughout AM-NPs development, several pilot studies were conducted to enhance their sustained release activity. Analysis of variance (ANOVA) was used to establish the statistical validity of polynomial equations produced by Design Expert software version 11. A predictor equation with interactive and polynomial terms to assess the responses is obtained by fitting a multiple linear regression statistical model to a 3^2-factorial design. We chose independent variables such as the concentrations of polyvinyl alcohol and gellan gum, because we found that they significantly affected the EE and DR during these batches [24]. A 3-level 2-factor design was employed to create contour plots of the responses and produce a second order polynomial equation [25-26]. Using Design Expert software, the best-fitting mathematical model was chosen by comparing a number of statistical parameters, including the coefficient of variation (CV), multiple correlation coefficient (R2), adjusted multiple correlation coefficient (adjusted R2), and predicted residual sum of squares. The significance level was set at $p<0.05$. Equations were transformed into three-dimensional response surface graphs using Design Expert software. The gellan gum concentration (X1) and polyvinyl alcohol concentration (X2) were selected as independent variables. Encapsulation efficiency (EE) Y1 (%) and Drug release (DR) Y2 (%) were selected as dependent parameters. A full-model second-order polynomial equation was constructed utilizing several regressions and the updated values of the independent and dependent variables [27].

Characterization:

Entrapment Efficiency: The following formula was used to determine the amount of entrapped Artemether in AM-NPs [28]:

$$\frac{D}{T} \times 100 \ldots\ldots \mathbf{eq(1)}$$

Where,

D=Weight of Drug determined, *T*=Weight of total drug added.

FT-IR: To evaluate the interaction between the various formulation components, FT-IR analysis was performed. Using an FTIR spectrophotometer (Perkin-Elmer, USA), materials were analyzed. FTIR analysis was performed on pure AM, GG, and AM-NPs using the KBr pellet technique. The sample was combined with KBr and manually pressed into a CD. The 4000–400 cm-1 range of the spectrum was analyzed [29].

XRD: XRD analysis was used to determine whether the material, which includes Pure AM, GG, and AM-NPs was amorphous or crystalline. [30-31] the diffraction angle 2θ was 10-800 and the scanning rate was 10/min. Cu Kα at 0.154 nm and a monochromator voltage of 40 kV were used to gather the results. In the region $5°<2\theta$, the diffraction pattern was identified.

Differential Scanning Calorimetry (DSC): Using DSC (DSC-60, Shimadzu, Kyoto, Japan), the thermal properties of the powdered samples of Pure AM, GG, and AM-NPs were investigated [32]. To determine the physical state of AM contained within the produced nanoparticles, DSC was performed. After precisely weighing each sample, they were all placed in an aluminium pan and kept at 10ºC min−1 between 40 and 250ºC[33].

Particle size distribution: The Malvern Zeta sizer ZS 200 was used to disperse the sample in water in order to determine the particle size distribution of Pure AM, GG, and AM-NPs. Using a Malvern Zetasizer (Nano ZS90, Malvern Instruments Ltd., U.K.), the Dynamic Light Scattering (DLS) technique was used to assess particle size, Zeta Potential (ZP), and PDI (Polydispersity Index). The samples were diluted ten times with distilled water to create a homogenous dispersion, which was used to measure the particle size, PDI, and Zeta potential [34].

***In-Vitro* Drug Release:** Dialysis membranes were used in in vitro release experiments. The dialysis bag (molecular weight cut off 20 kDa, pore size 0.2 µm) was filled with 100 ml of phosphate buffered saline (PBS) at pH 7.4 after the AM-NPs (equal to 25 mg of medication) were dissolved in 10 ml of distilled water. A magnetic stirrer was used to continually agitate the medium at 50 rpm while maintaining a temperature of 37±0.5°. Over the course of 48 hours, 5 ml of the sample was taken out at different times, and each sampling was conducted with new phosphate buffered saline (PBS) at a pH of 7.4. The UV-Visible spectrometer at 212 nm was used to measure the amount of medication emitted. [35-37]

Result and Discussion:

Entrapment Efficiency: The drug entrapment efficiency for respective experimental batches is shown in **Table 1**. The drug entrapment efficiency of all formulations in the ranges of 82.98-91.78 %. F2 batch having gellan gum and polyvinyl alcohol concentration at 0.05 % each shows lesser entrapment efficiency.

FT-IR: Figure 1 shows the FT-IR spectra of pure AM, GG and AM-NPs. FTIR spectra of artemether (ARTM) indicated the presence of four characteristic peaks of C–H stretching vibrations at 2698 cm^{-1}, 2813 cm^{-1}, 2910 cm^{-1}, C–H aromatic stretching at 3288 cm^{-1} and C–O–O–C bending vibrations at 1119 cm^{-1}, C–O–C stretching vibrations at 1036 cm^{-1} and 1277.83 cm^{-1}, and C–H bending vibrations at 1452 cm^{-1}[38].The spectra of gellan gum shows characteristic peaks at 1599cm^{-1} (shows C–O stretching vibrations), 1404cm^{-1} (O-H bending vibration) and 1021cm^{-1} (C-O-C stretching).In the spectrum of AM-NPs, various characteristic peaks of pure AM were appeared without any significant deviation of these peaks. It shows no interaction.

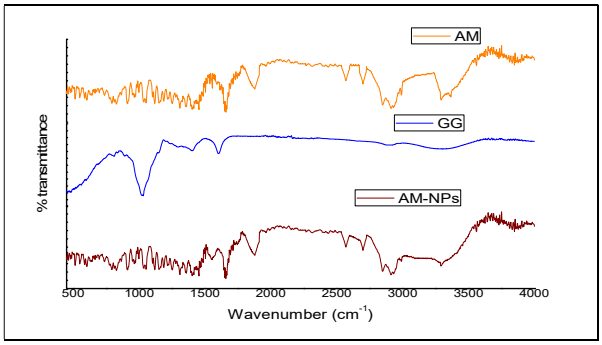

Figure 1. FTIR spectra of AM, GG and AM-NPs.

(**AM**- Artemether, **GG**- Gellan gum, **AM-NPs**-Artemether -Gellan gum Nanoparticles)

XRD: Figure 2 shows the XRD patterns of pure AM, and AM-NPs. The crystallinity peak in the XRD spectra of AM was sharp and intense. XRD patterns of pure AM shows 2Θ at10.85°, 12.81°, 14.16°, 15.71°, 17.09°, 19.43°, 23.03°, 27.83° and 41.57°, indicating a crystallinity[39]. On the other hand, XRD spectra of AM-NPs showed a less intense peak of crystallinity as compared to the pure drug. As a result of the produced AM-NPs has in an amorphous state and spread in gellan gum.

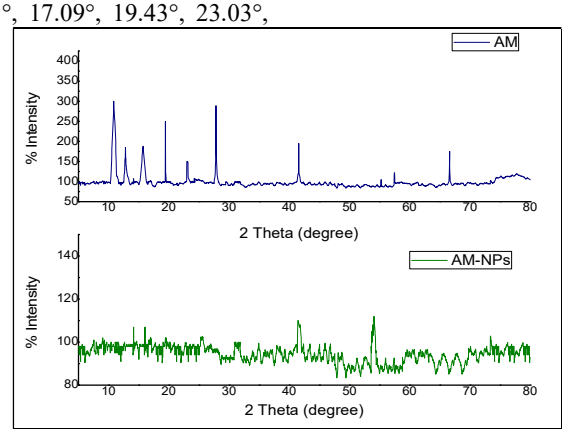

Figure 2. XRD spectra of AM and AM-NPs.

DSC: This test was performed to investigate the interaction between drugs and carriers. DSC thermograms of pure AM, GG and AM-NPs are shown in Figure 3. A sharp endothermic peak at 89 ^{o}C was observed in the thermogram of AM, which corresponds to the melting point of the pure AM. [40] In DSC thermograms of GG, a broad endothermic peak is observed between 50-60 ^{0}C, which corresponds to melting point of pure GG. The thermogram of AM-NPs indicates melting peaks of both pure AM and pure GG, which indicates no interaction between AM and GG. Slight decrease in thermograms intensity in AM may be due to decrease in crystallinity of drug in AM-NPs.

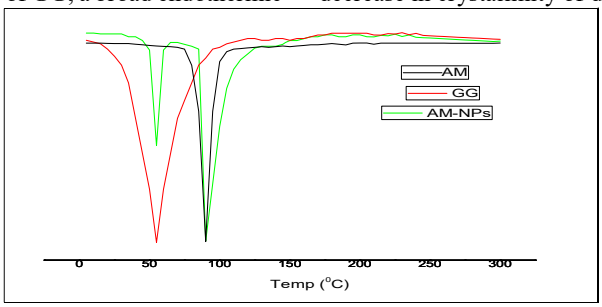

Figure 3. DSC thermogram of AM, GG and AM-NPs.

Particle size distribution: The mean size (d. nm) of AM and AM-NPs was about 729.7 nm and 263.3 Figure 4. In pure form of AM, it has higher particle size than AM in nanoparticles. It indicates that particle size in optimized formulation is in nanoparticles ranges. The zeta potential of optimized formulation was found -15.8 (mV) it indicates good stability

.

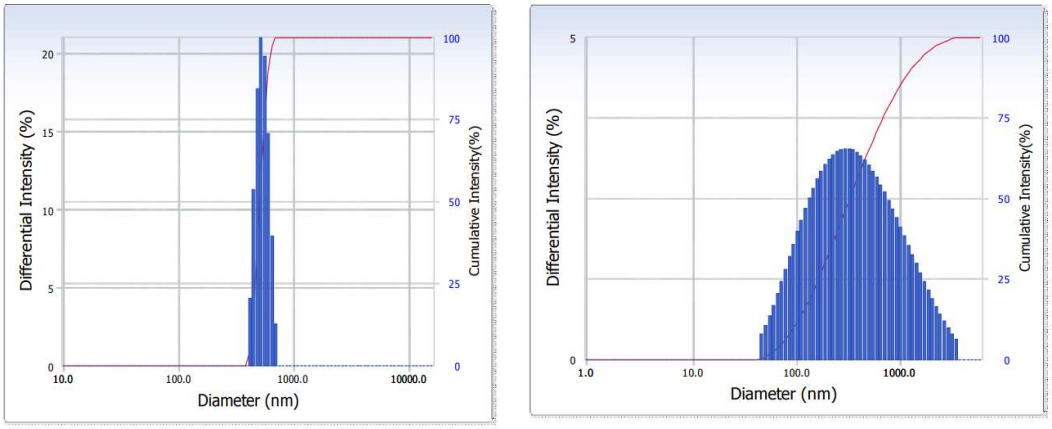

(a) (b)

Figure 4. Average size (d. nm) of (a) pure AM, (b) AM-NPs.

In-Vitro Drug Release: These studies were performed to determine the % of drug release from the AM-NPs (See **Figure 5**). The drug release in phosphate buffered saline (PBS) at pH 7.4 was performed for 12 hrs. time duration . The drug release of all 13 prepared AM-NPs shows about 87.09 -98.26 % for 12 hrs. duration. The DR of pure AM shows drug release of about 90 % within 8 hrs.

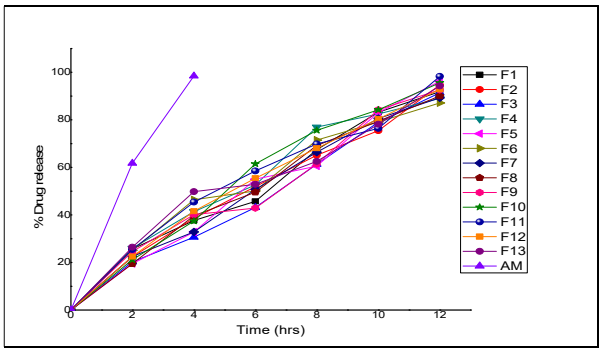

Figure 5. Dissolution profiles pure AM and each 13 batches of AM-NPs.

*Author for Correspondence: amrita.bharti@sharda.ac.in

Optimization: Design-Expert 11.0 was used to build the mathematical link between the variables, and its capacity to estimate response variables and interact to provide clear effects on responses was then assessed. The Design-Expert was used to examine the outcomes for the nine formulations and compare their formulations to other models. However, the best fit was noted. A 3^2 response surface methodology was used to ascertain the impact of independent factors (X1, X2) on dependent variables (Y1, Y2) with the fewest number of experimental trials [41]. To assess the impact of these independent parameters, counter plots in two dimensions (Figure 6a, 7a) and three dimensions (Figure 6b, 7b) were created [42]. Thirteen batches were carried out in order to produce AM-NPs. The effects of two independent factors (A, B) on the dependent variables (Y1, Y2) were investigated statistically using a 3^2-factorial design [43]. For the first dependent factor, Y1, or EE, the second order polynomial equation was also produced. It was like this:

$$Y_1 = 88.1617 + 2.03667.\ x_1 + -1.65667.\ x_2 + 0.4775.x_1x_2 + 2.08897.\ x_1^2 + -2.7510.\ x_2^2 \ldots\ldots \text{eq (2)}$$

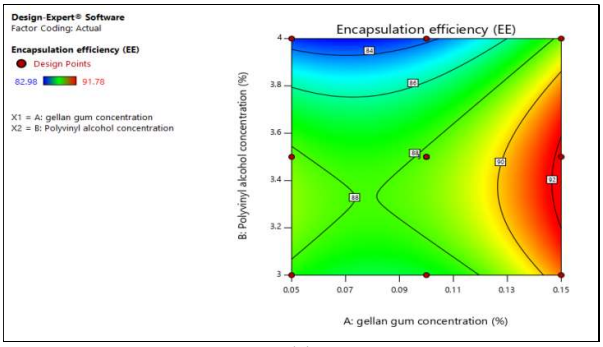

(a)

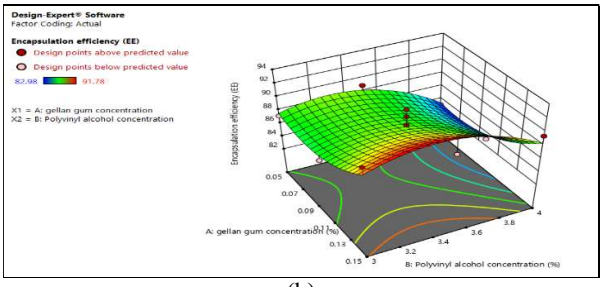

(b)

Figure 6. 2D contour (a) and 3D plot (B) for entrapment efficiency.

Additionally, the polynomial equation for Y2, or DR, the second dependent factor, was derived. The second-order polynomial equation that was obtained was

$$Y_2 = 93.2492 + -0.108333.\ x_1 + 3.42167.\ x_2 \ldots\ldots \text{eq (3)}$$

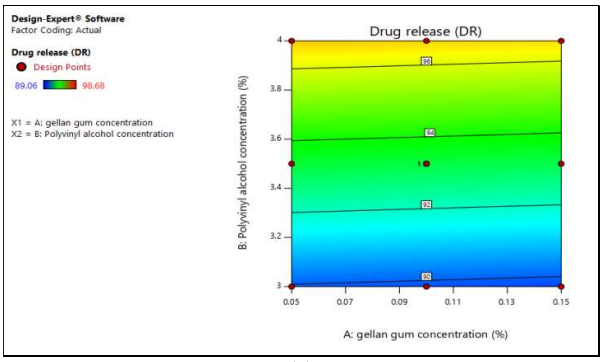

(a)

*Author for Correspondence: amrita.bharti@sharda.ac.in

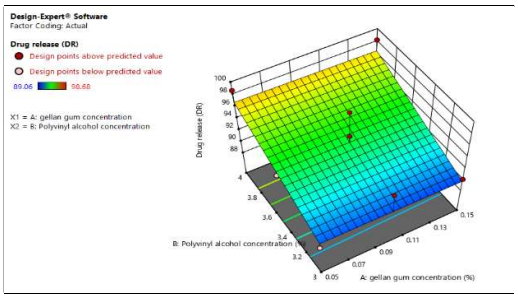

(b)

Figure 7.2D contour (a) and 3D plot (B) for drug release.

The correlation coefficient (R2) values for the Y1 and Y2 responses were 0.7494 and 0.3815, respectively, suggesting a quadratic equation and linear model that provide a reasonable match (Table 2). For the EE (Y1) and DR (Y2) responses, the following equations were discovered. Positive and negative numbers, respectively, indicate antagonistic and synergistic effects in the aforementioned equations [44-45]. Table 3 shows the ANOVA for the response of models Y1 and Y2. The equation indicates that entrapment efficiency (Y1) was influenced by the independent variables x_1, x_2, x_1^2, x_2^2 and x_1x_2. Similarly, the drug release (Y2) response, which is a quadratic equation, was influenced only by the independent components $x_1 and\ x_2$. These independent parameters had a substantial effect on both entrapment efficiency (EE) and drug release (DR) at P<0.05[46]. Both models were significant at P<0.05, with corresponding F-values of 4.19 and 4.70. R2, adjusted R2, predicted R2, SD, and even the regression equation produced for each answer are included in the ANOVA values. The model terms were statistically significant, indicating that the likelihood of mistake is less than zero, when the p-value was less than 0.05. Table 4 shows the actual, expected, and residual values for each response variable together with the diagnostic case statistics. The prediction error was calculated by comparing the experimental value with the expected value. The actual and projected values differed less, indicating that the model was well-fitted. [47-48]

Table 2. Regression analysis for responses *Y*1 and *Y*2:

Source	Std. Dev.	R^2	Adjusted R^2	Predicted R^2	PRESS	Remark
Y1 Response						
Linear	2.18	0.4648	0.3578	0.1235	77.98	
2FI	2.28	0.4751	0.3001	0.0196	87.23	
Quadratic	**1.78**	**0.7494**	**0.5704**	**-0.1476**	**102.10**	**Suggested**
Cubic	1.80	0.8185	0.5645	-3.0965	364.45	
Y2 Response						
Linear	**0.4846**	**0.3815**	**0.2538**	**108.29**	**0.4846**	**Suggested**
2FI	0.4882	0.3176	-0.0100	146.56	0.4882	
Quadratic	0.5454	0.2207	-0.4793	214.66	0.5454	
Cubic	0.6381	0.1314	0.3099	100.14	0.6381	

Table 3. ANOVA for *Y*1 and *Y*2:

Source	Sum of Squares	df	Mean Square	F-value	p-value	Remark
Response Y1						
Model	66.67	5	13.33	4.19	0.0442	**Significant**
x_1	24.89	1	24.89	7.81	0.0267	
x_2	16.47	1	16.47	5.17	0.0572	
x_1x_2	0.9120	1	0.9120	0.2864	0.6091	
x_1^2	12.05	1	12.05	3.78	0.0928	
x_2^2	20.90	1	20.90	6.56	0.0375	
Response Y2						
Model	70.32	2	35.16	4.70	0.0364	**Significant**
x_1	0.0704	1	0.0704	0.0094	0.9246	
x_2	70.25	1	70.25	9.39	0.0119	

Table 4. Diagnostics case statistics for various response variables:

Run Order	Actual Value	Predicted Value	Residual	Actual Value	Predicted Value	Residual
Response Y1				**Response Y2**		
F1	88.42	88.16	0.2583	91.87	93.25	-1.38
F2	82.98	83.33	-0.3488	98.68	96.78	1.90
F3	90.14	92.29	-2.15	91.39	93.14	-1.75
F4	87.23	87.60	-0.3672	89.06	89.94	-0.8759
F5	87.44	88.16	-0.7217	98.22	93.25	4.97
F6	91.78	90.72	1.06	90.09	89.72	0.3708
F7	90.67	88.16	2.51	89.28	93.25	-3.97
F8	86.05	88.16	-2.11	90.06	93.25	-3.19
F9	88.93	88.21	0.7160	92.65	93.36	-0.7076
F10	83.02	83.75	-0.7340	95.57	96.67	-1.10
F11	89.44	88.36	1.08	98.26	96.56	1.70
F12	86.37	87.07	-0.6974	92.83	89.83	3.00
F13	89.66	88.16	1.50	94.28	93.25	1.03

Conclusion:

Malaria is a global health priority with more than 3 billion people at risk. Effective treatment of malaria is hampered by the rapid development and dissemination of resistance to all known classes of antimalarial drugs. One of the earliest antimalarial drugs is artemether. It is more effective against parasites that are resistant to other drugs. It belongs to the class II biopharmaceuticals, which are poorly soluble and have high permeability. Its half-life of two to three hours is extremely brief. Artemether traditional dose form requires regular dosing. To prevent frequent dosage, prolonged release Artemether-gellan gum nanoparticles are successfully prepared in this work. Using the emulsion cross-linking technique, Artemether-gellan gum nanoparticles were created. The 3-level 2-factor design procedure was used to optimize the concentrations of Polyvinyl alcohol and gellan gum. Using a 3^2-factorial design, the statistical effects of two independent factors (X1, X2) on the dependent variables (Y1, Y2) were examined. The Y1 and Y2 responses' respective correlation coefficients (R2) were 0.7494 and 0.3815, indicating a linear equation and quadratic model that offer a satisfactory match. With matching F-values of 4.19 and 4.70, both models were significant at $P<0.05$. Drug entrapment efficiency ranged from 82.98 to 91.78% for all formulations. There is no interaction between AM-NPs FTIR and DSC thermograms. The XRD peaks indicate that the prepared AM-NPs are in an amorphous state. The zeta potential of -15.8 (mV) for the enhanced formulation indicates good stability. The drug release of all 13 generated AM-NPs varies between 87.09 and 98.26 percent over a 12-hour period. The developed Artemether-gellan gum nanoparticle combination provides a 12-hour sustained release effect and resolves common Artemether dosage problems.

Ethical Statement:

Ethics approval and consent to participate: Not applicable.

Consent for publication: Not applicable.

Availability of data and materials: No additional data and materials are associated with this article to support the findings of the article.

Competing interests: Not applicable.

Finding: Not applicable.

Author contributions: All authors contributed to the study conception and design. All authors also read and approved the final manuscript.

Acknowledgements: The authors are grateful to Department of Pharmacy, IES University, Bhopal, Madhya Pradesh, India for providing infrastructure to carry out this work.

REFERENCE

1. Fikadu M, Ashenafi E. Malaria: an overview. Infection and Drug Resistance. 2023 Dec 31:3339-47.
2. Mulebeke R, Yeka A, van Geertruyden JP. Enhancing malaria elimination in high-transmission settings: the synergy of concurrent vector control and chemotherapy. Malaria Journal. 2025 Apr 1; 24(1):105.
3. Ahamed MF, Nahiduzzaman M, Mahmud G, Shafi FB, Ayari MA, Khandakar A, Abdullah-Al-Wadud M, Islam SR. Improving Malaria diagnosis through interpretable customized CNNs architectures. Scientific Reports. 2025 Feb 22; 15(1):6484.
4. Zheng D, Tian P, Yan G, Lin Z, Zhou H, Liu X, Chen J, Liu Q, Lin H. Stratified vector control and proactive cross border collaboration for sustaining malaria elimination in Yunnan, China. bmj. 2025 Apr 22; 389.
5. Daily JP, Minuti A, Khan N. Diagnosis, treatment, and prevention of malaria in the US: a review. Jama. 2022 Aug 2; 328(5):460-71.
6. Andrade MV, Noronha K, Diniz BP, Guedes G,

Carvalho LR, Silva VA, Calazans JA, Santos AS, Silva DN, Castro MC. The economic burden of malaria: a systematic review. Malaria journal. 2022 Oct 5; 21(1):283.

7. Poespoprodjo JR, Douglas NM, Ansong D, Kho S, Anstey NM. The Malaria. The Lancet (British edition). 2023 Dec 16; 402(10419):2328-45.
8. Peto TJ, Tripura R, Callery JJ, Lek D, Nghia HD, Nguon C, Thuong NT, van der Pluijm RW, Dung NT, Sokha M, Van Luong V. Triple therapy with artemether–lumefantrine plus amodiaquine versus artemether–lumefantrine alone for artemisinin-resistant, uncomplicated falciparum malaria: an open-label, randomised, multicentre trial. The Lancet Infectious Diseases. 2022 Jun 1; 22(6):867-78.
9. Goodwin J, Kajubi R, Wang K, Li F, Wade M, Orukan F, Huang L, Whalen M, Aweeka FT, Mwebaza N, Parikh S. Persistent and multiclonal malaria parasite dynamics despite extended artemether-lumefantrine treatment in children. Nature Communications. 2024 May 7; 15(1):3817.
10. Ocan M, Nakalembe L, Otike C, Omali D, Buzibye A, Nsobya S. Pharmacopeial quality of artemether–lumefantrine anti-malarial agents in Uganda. Malaria Journal. 2023 May 26; 22(1):165.
11. Rong G, Weng W, Huang J, Chen Y, Yu X, Yuan R, Gu X, Wu X, Cai Y, Han P, Shao M. Artemether alleviates diabetic kidney disease by modulating amino acid metabolism. BioMed research international. 2022; 2022(1):7339611.
12. Nnamani PO, Ugwu AA, Nnadi OH, Kenechukwu FC, Ofokansi KC, Attama AA, Lehr CM. Formulation and evaluation of transdermal nanogel for delivery of artemether. Drug Delivery and Translational Research. 2021 Aug; 11:1655-74.
13. Beach MA, Nayanathara U, Gao Y, Zhang C, Xiong Y, Wang Y, Such GK. Polymeric nanoparticles for drug delivery. Chemical Reviews. 2024 Apr 16; 124(9):5505-616.
14. Elmowafy M, Shalaby K, Elkomy MH, Alsaidan OA, Gomaa HA, Abdelgawad MA, Mostafa EM. Polymeric nanoparticles for delivery of natural bioactive agents: recent advances and challenges. Polymers. 2023 Feb 23; 15(5):1123.
15. Pulingam T, Foroozandeh P, Chuah JA, Sudesh K. Exploring various techniques for the chemical and biological synthesis of polymeric nanoparticles. Nanomaterials. 2022 Feb 8; 12(3):576.
16. Gomes D, Batista-Silva JP, Sousa A, Passarinha LA. Progress and opportunities in Gellan gum-based materials: A review of preparation, characterization and emerging applications. Carbohydrate Polymers. 2023 Jul 1; 311:120782.
17. Abdl Aali RA, Al-Sahlany ST. Gellan gum as a unique microbial polysaccharide: Its characteristics, synthesis, and current application trends. Gels. 2024 Mar 6; 10 (3):183.
18. Zhou TQ, Wang XC, Gao LY, Yan JN, Wu HT. Construction and properties of curdlan gum/gellan gum binary composite gel system. Food Hydrocolloids. 2024 Mar 1; 148:109391.
19. Dev MJ, Warke RG, Warke GM, Mahajan GB, Patil TA, Singhal RS. Advances in fermentative production, purification, characterization and applications of gellan gum. Bioresource Technology. 2022 Sep 1; 359:127498.
20. Feketshane Z, Alven S, Aderibigbe BA. Gellan gum in wound dressing scaffolds. Polymers. 2022 Sep 30; 14(19):4098.
21. Prakash SJ, Santhiagu A, Jasemine S. Preparation, characterization and in vitro evaluation of novel gellan gum-raloxifene HCl nanoparticles. J Pharm BioSci. 2014 Jul; 2:63-71.
22. Dodi G, Pala A, Barbu E, Peptanariu D, Hritcu D, Popa MI, Tamba BI. Carboxymethyl guar gum nanoparticles for drug delivery applications: Preparation and preliminary in-vitro investigations. Materials Science and Engineering: C. 2016 Jun 1; 63:628-36.
23. Kandav G, Lochab AK, Sharma T. Design and Characterization of Timolol Loaded Gellan Gum Nanoparticles for Improved Ocular Drug Delivery. Indian Journal of Pharmaceutical Education and Research. 2024 Jun 21; 58(3):751-9.
24. Abbas Z, Marihal S. Gellan gum-based mucoadhesive microspheres of almotriptan for nasal administration: Formulation optimization using factorial design, characterization, and: in vitro: evaluation. Journal of Pharmacy and Bioallied Sciences. 2014 Oct 1; 6(4):267-77.
25. Nandi G, Nandi AK, Khan NS, Pal S, Dey S. Tamarind seed gum-hydrolyzed polymethacrylamide-g–gellan beads for extended release of diclofenac sodium using 32 full factorial design. International journal of biological macromolecules. 2018 Jul 15; 114:214-25.
26. Shukla S, Favata J, Srivastava V, Shahbazmohamadi S, Tripathi A, Shukla A. Effect of polymer and ion concentration on mechanical and drug release behavior of gellan hydrogels using factorial design. Journal of Polymer Science. 2020 May 15; 58(10):1365-79.
27. Kumar S, Kaur P, Bernela M, Rani R, Thakur R. Ketoconazole encapsulated in chitosan-gellan gum nanocomplexes exhibits prolonged antifungal activity. International journal of biological macromolecules. 2016 Dec 1; 93:988-94.

28. Castro PM, Baptista P, Madureira AR, Sarmento B, Pintado ME. Combination of PLGA nanoparticles with mucoadhesive guar-gum films for buccal delivery of antihypertensive peptide. International Journal of Pharmaceutics. 2018 Aug 25; 547(1-2):593-601.
29. Villarreal-Otalvaro C, Coburn JM. Fabrication methods and form factors of gellan gum-based materials for drug delivery and anti-cancer applications. ACS Biomaterials Science & Engineering. 2021 Dec 13; 9(7):3832-42.
30. Nair AB, Shah J, Aljaeid BM, Al-Dhubiab BE, Jacob S. Gellan gum-based hydrogel for the transdermal delivery of nebivolol: Optimization and evaluation. Polymers. 2019 Oct 16; 11(10):1699.
31. Patel AK, Mishra MK, Gupta J, Ghoshal S, Gupta R, Kushwaha K. Guar Gum-based floating microspheres of repaglinide using 32 factorial design: fabrication, optimization, characterization, and in vivo buoyancy behavior in albino rats. ASSAY and Drug Development Technologies. 2021 Mar 1; 19(2):63-74.
32. Dhar S, Mali V, Bodhankar S, Shiras A, Prasad BL, Pokharkar V. Biocompatible gellan gum-reduced gold nanoparticles: cellular uptake and subacute oral toxicity studies. Journal of Applied Toxicology. 2011 Jul; 31(5):411-20.
33. Yadav KS, Sawant KK. Formulation optimization of etoposide loaded PLGA nanoparticles by double factorial design and their evaluation. Current drug delivery. 2010 Jan 1; 7(1):51-64.
34. Bhavsar MD, Tiwari SB, Amiji MM. Formulation optimization for the nanoparticles-in-microsphere hybrid oral delivery system using factorial design. Journal of controlled release. 2006 Jan 10; 110(2):422-30.
35. Asif AH, Desu PK, Alavala RR, Rao GS, Sreeharsha N, Meravanige G. Development, statistical optimization and characterization of fluvastatin loaded solid lipid nanoparticles: a 32 factorial design approach. Pharmaceutics. 2022 Mar 8; 14(3):584.
36. Ranjan A, Jha PK. Experiments and modeling of controlled release behavior of commercial and model polymer-drug formulations using dialysis membrane method. Drug delivery and translational research. 2020 Apr; 10:515-28.
37. Wallenwein CM, Nova MV, Janas C, Jablonka L, Gao GF, Thurn M, Albrecht V, Wiehe A, Wacker MG. A dialysis-based in vitro drug release assay to study dynamics of the drug-protein transfer of temoporfin liposomes. European Journal of Pharmaceutics and Biopharmaceutics. 2019 Oct 1; 143:44-50.
38. Ansari MT, Hussain A, Nadeem S, Majeed H, Saeed-Ul-Hassan S, Tariq I, Mahmood Q, Khan AK, Murtaza G. Preparation and Characterization of Solid Dispersions of Artemether by Freeze-Dried Method. BioMed research international. 2015; 2015(1):109563.
39. Xu J, Singh V, Yin X, Singh P, Wu L, Xu X, Guo T, Sun L, Gui S, Zhang J. Solvents effects on crystallinity and dissolution of β-artemether. Drug development and industrial pharmacy. 2017 Mar 4; 43(3):372-8.
40. Fule RA, Meer TS, Sav AR, Amin PD. Artemether-Soluplus Hot-Melt Extrudate Solid Dispersion Systems for Solubility and Dissolution Rate Enhancement with Amorphous State Characteristics. Journal of pharmaceutics. 2013; 2013(1):151432.
41. Derakhshandeh K, Erfan M, Dadashzadeh S. Encapsulation of 9-nitrocamptothecin, a novel anticancer drug, in biodegradable nanoparticles: factorial design, characterization and release kinetics. European journal of pharmaceutics and biopharmaceutics. 2007 Apr 1; 66(1):34-41.
42. Amin H, Osman SK, Mohammed AM, Zayed G. Gefitinib-loaded starch nanoparticles for battling lung cancer: Optimization by full factorial design and in vitro cytotoxicity evaluation. Saudi Pharmaceutical Journal. 2023 Jan 1; 31(1):29-54.
43. Akl MA, Kartal-Hodzic A, Oksanen T, Ismael HR, Afouna MM, Yliperttula M, Samy AM, Viitala T. Factorial design formulation optimization and in vitro characterization of curcumin-loaded PLGA nanoparticles for colon delivery. Journal of Drug Delivery Science and Technology. 2016 Apr 1; 32:10-20.
44. Ghasemian E, Vatanara A, Rouholamini Najafabadi A, Rouini MR, Gilani K, Darabi M. Preparation, characterization and optimization of sildenafil citrate loaded PLGA nanoparticles by statistical factorial design. DARU Journal of Pharmaceutical Sciences. 2013 Dec; 21:1-10.
45. Petkar KC, Chavhan S, Kunda N, Saleem I, Somavarapu S, Taylor KM, Sawant KK. Development of novel octanoyl chitosan nanoparticles for improved rifampicin pulmonary delivery: optimization by factorial design. AAPS PharmSciTech. 2018 May; 19:1758-72.
46. Carraro TC, Khalil NM, Mainardes RM. Amphotericin B-loaded polymeric nanoparticles: formulation optimization by factorial design. Pharmaceutical Development and Technology. 2016 Feb 17;21(2):140-6
47. Teja SS, Damodharan N. 23 full factorial model for particle size optimization of methotrexate loaded chitosan nanocarriers: a design of experiments (DoE) approach. BioMed research international. 2018; 2018(1):7834159.

48. Attia MS, Radwan MF, Ibrahim TS, Ibrahim TM. Development of carvedilol-loaded albumin-based nanoparticles with factorial design to optimize in vitro and in vivo performance. Pharmaceutics. 2023 May 6; 15(5):1425